

CHALMERS

Energy Conversion

Mechanical and Vehicular Engineering – Chalmers University of Technology

Report A 97-221

**Fuel Loading of a Fluidized Bed
Combustor Burning Bituminous
Coal, Peat or Wood Chips**

**L.-E. Åmand
A. Lyngfelt
M. Karlsson
B. Leckner**

Revised December 1999

ABSTRACT

Characterisation of gas- and particle phases in the combustion chamber of a commercial size circulating fluidized bed (CFB) boiler has been carried out during tests with three different fuels: bituminous coal, peat and wood chips, for typical operating conditions of a CFB boiler. The evaluation of the test results aims at presenting data on the fuel loading in parallel with the vertical profiles of oxygen concentration to be used for validation of models and for modelling of the fuel loading. The measurements show that the char loading during peat combustion is 13% of the amount found during coal combustion. Wood combustion results in even less char, only 3.5% of the concentration during coal combustion. For all fuels, more than 80% of the mass of char is retained in the lower part of the combustion chamber, below 2 meter from the bottom plate. The oxygen concentration profiles show large variations over the cross section for all three fuels, explained as an effect of insufficient penetration of secondary air in combination with partial plugging of some of the secondary air nozzles. In the peat and wood cases some of the variation over the cross section is caused by the high volatile content of the fuel in combination with a fuel supply from only one of the furnace walls.

Key words: Fluidized-bed combustion, circulating fluidized bed boiler, fuel loading, oxygen concentration profiles

1 INTRODUCTION

Fuel loading is a key parameter for the understanding of the nitrogen chemistry in a fluidized bed boiler and for the dynamics of the operation of the boiler.

The aim of the present project is to present values of fuel loading from tests carried out on the circulating fluidized bed (CFB) boiler at Chalmers University of Technology, operated with quite different fuels, such as bituminous coal, peat and wood chips. The paper gives the experimental background for the determination of the fuel load during coal, peat and wood chips combustion as well as the oxygen concentration profiles in the combustion chamber needed for combustion modelling. The results presented have a value themselves as an example, but the purpose of the presentation is to give basis of data for modelling. This is the reason why detailed measurements results and boiler status are included. The experimental results presented have been used in a previous study concerning the progress of combustion in the combustion chamber, Lyngfelt et al., 1996.

2 EXPERIMENTAL

2.1 Boiler

The tests were run on the 12 MW_(th) CFB boiler at Chalmers University of Technology (Fig. 2.1.1). The boiler is built in the form of a commercial unit with the combustion chamber (1) made up of membrane tube walls with a square cross-section of about 2.5 m² and a height of 13.6 meter with the cyclone outlet beginning at 9.3 m. Fuel is fed to the bottom of the combustion chamber (1) through a fuel chute (2). Primary air (3) is introduced through nozzles in the bottom plate and secondary air can be injected through several inlets, consisting of sets of nozzles located along the height of the combustion chamber

at various heights as indicated by the arrows in Fig.2.1.1.

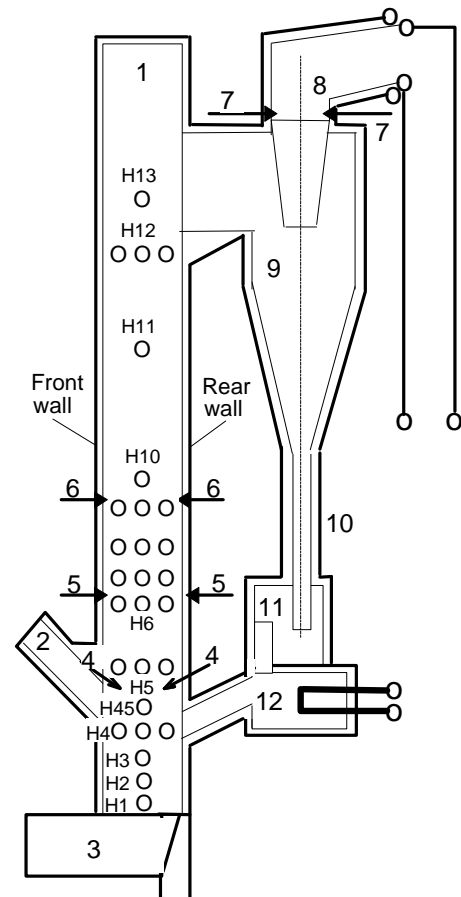


Fig. 2.1.1 The 12-MW_{th} CFB boiler at Chalmers University of Technology (1) combustion chamber; (2) fuel feed chute; (3) air plenum; (4) secondary air inlet at 2.1m; (5) secondary air inlet at 3.7m; (6) secondary air inlet at 5.4m; (7) secondary air inlet into cyclone exit duct; (8) cyclone exit duct (9) cyclone; (10) particle return leg; (11) particle seal; (12) heat exchanger. Measurement ports (H1 to H13) on the right boiler wall are indicated.

The lowest secondary air inlet (4) is located at 2.1 meter, the second (5) at 3.7 meter and the third and highest (6) at 5.4 meter. It is also possible to supply air to the outlet of the cyclone (7), (8) and thereby to operate both the boiler and the cyclone at the stoichiometric conditions desired. Entrained bed material is captured in the hot refractory-lined cyclone (9) and returned to the combustion chamber through the return leg (10) and particle seal (11). The bed temperature is controlled by heat transfer to the membrane-tube walls and by a heat exchanger (12) located in communication with the particle seal and by recycled flue gas which is mixed with the primary air in the air plenum (3) before entering the combustion chamber.

Also indicated in Fig. 2.1.1 are the ports in the right boiler wall. These ports make it possible to penetrate into the combustion chamber with various types of measurement probes in order to characterise the gas- and particle phases of the furnace. Not seen in Fig. 2.1.1 is the ash classifier located in connection to the bottom ash removal. The ash classifier works in a continuous mode with the aim of removing only the coarse fractions of the bed material such as stones and large ash particles. The fines and the original silica sand particles are blown back to the combustion chamber.

2.1.1 Secondary Air Nozzles

In the tests presented in this report only the lowest secondary air inlet was used. Secondary air then penetrates from both the front and back wall through 13 nozzles, 7 in the front wall and 6 in the back wall

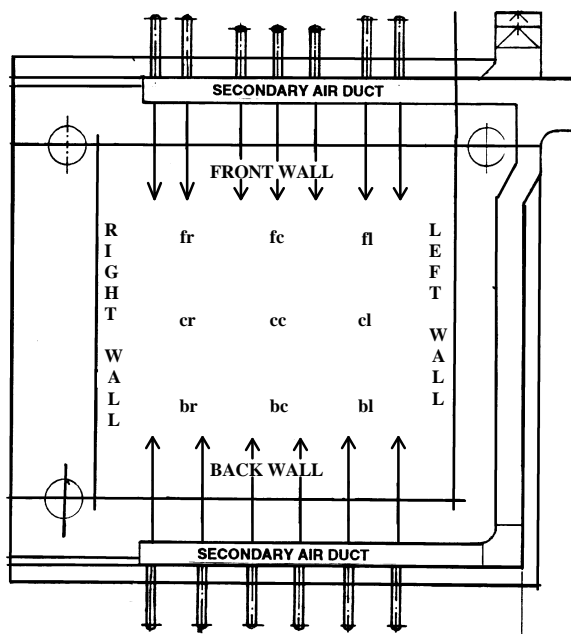


Fig. 2.1.1.1 Detail of secondary air supply equipment with the locations of the nozzles in the boiler. Measurement positions with gas extraction probe are indicated.

Fig. 2.1.1.1. The distance between the nozzles is 0.15 to 0.25 meter and they are all inclined downwards 45°. The diameter of the nozzle outlet is between 0.07 and 0.1 meter giving a total nozzle area of 0.057m². The secondary air flow used resulted in an average nozzle exit velocity of 20 m/s. This is not sufficient to achieve the momentum needed for complete penetration into the centre of the combustion chamber 0.72 meter from the wall. In addition, visual inspection of the nozzles during turn down periods of the boiler showed a partial plugging of the nozzles. Even if the nozzles were carefully rinsed prior to start-up of the boiler, an uncertainty regarding the number of nozzles in efficient use during measurement remains. This could affect the results of the gas concentration measurements in the combustion chamber shown later.

Apart from the primary and secondary-air nozzles, air also enters the combustion chamber from the particle seal and ash classifier. These inlets are both located in the back wall: the cyclone leg inlet at a height of 0.99 meter, 0.180 meter from left wall and with an area of 0.105 m². The ash classifier inlet is located at a height of 1.29 meter, 0.2 meter from the right wall with an area of 0.014 m². The air flows through these holes are in the range 0.9-2.6 and 1.5-2.0 times the flow through a single secondary air nozzle. With the areas given, these flows enter the combustion chamber with velocities of between 3-7.6 and 42.8-57.4 m/s respectively dependent on which of the three fuels that was used.

2.2 Gas Analysis System

The Chalmers boiler is equipped with two sets (A and B) of on-line conventional flue-gas analysers for continuous monitoring of O₂, CO, SO₂, NO and N₂O in the stack and O₂, NO, CO, CO₂, SO₂, hydrogen (H₂) and total hydrocarbons (HC-tot) in the combustion gas from the gas analysis probe. Apart from the on-line analysers, an FTIR, and a gas chromatograph equipped with a mass spectrometer (GC-MS) are integrated parts of the B-system. For more details, see Karlsson et al., 1996. Of special interest in this project is the oxygen analyser of the B-system. This analyser from Hartmann & Braun utilises the paramagnetic principle and analyses the oxygen concentration on dry basis. The analyser was regularly calibrated before use in each measurement with the various fuels.

The gas sampling probe is shown in Fig. 2.2.1. This probe is designed for analysis of wet combustion gases which is important when, for example, NH₃ is to be analysed. The combustion gas first passes through a ceramic filter mounted at the tip of the probe, Fig. 2.2.2, protected and cooled by the cooling shield of the probe. The filter with a pore size of 100 microns is made of fused alumina particles bonded with a complex alumina borosilicate glass.

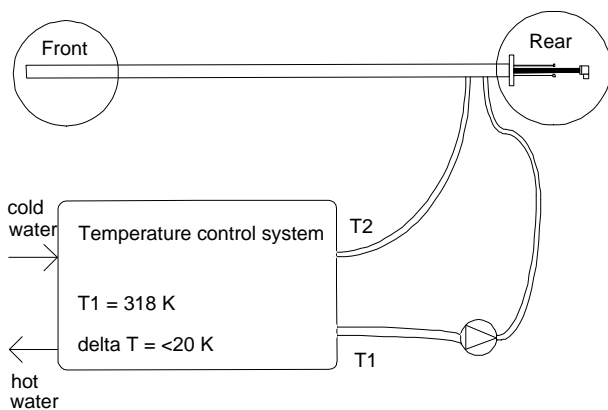


Fig. 2.2.1 Gas sampling probe used for analysis of hot gases from the combustion chamber.

This material should be temperature resistant up to 1100 °C. The filter is made by the Ferro Corporation under the name Kellundite. After passing the filter the combustion gas is transported through the centre-pipe which is electrically heated to approximately 200 °C, Fig. 2.2.3. In order to control the cooling of the centre-pipe the probe is cooled by heated water, Fig. 2.2.1, (temperature between 45 and 95 °C). Downstream of the probe the combustion gas is transported to the gas analysers through heated gas sampling lines. The ceramic filter is regularly cleaned from ash and bed material by back-flushing the probe with pressurised air.

2.3 The Suction Probes for Extraction of Bed Material

The normal procedure to take bed samples was to use an uncooled suction probe, where the sample was cooled to room temperature prior to removal from the probe. In one of the test series a cooled probe was used, where the sample was quenched by pure nitrogen prior to storage in sealed containers awaiting the analysis, Mattisson & Lyngfelt, 1995.

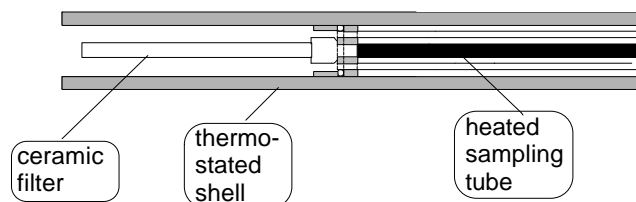


Fig. 2.2.2 Front part of the gas sampling probe.

The char content obtained with this new probe did not, however, differ significantly from those obtained with the uncooled probe. The samples higher up in the combustion chamber were taken by a third probe, a cooled suction probe, equipped with a small cyclone, as reported by Zhang et al., 1993. Some of the samples were sieved. With a proximate analyser (Mac 400 from Leco Corporation, USA) the char content in the solid samples could be determined as a mass loss after combustion of the char fraction with oxygen. By using the proximate analyser on each sieve fraction, the size distribution of the char fraction in the solid samples could be determined. The problem with this method is that the char fractions close to the size of the sand used as bed material are heavily diluted by sand and the concentration limit of the proximate analyser nearly is reached, which corresponds to a char content of 0.01%. This means that an uncertainty is introduced for those size fractions. Other uncertainties in the determination of the size of the char fraction occur for the largest fractions as well as for the smallest ones. There were only a few large particles present in each solid sample, and a collection of a representative amount of particles was difficult. For the smallest particles the problem is that they can be attached to larger ones during the sieving process and may not be separated properly. On the other hand fines can be produced during sieving, increasing the amount of char fines in relation to what was present in the sample prior to the sieving process.

2.4 The Tests

The operating conditions were those of a so called reference case corresponding to typical operating conditions of a CFB boiler, that is, a combustion

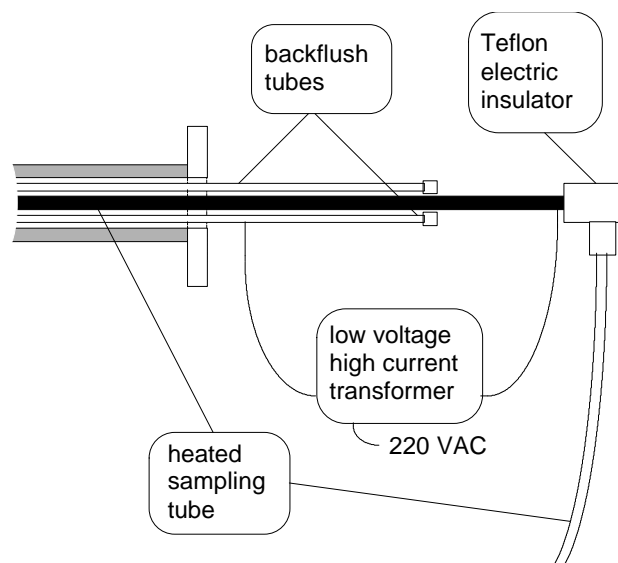


Fig. 2.2.3 Rear part of the gas sampling probe.

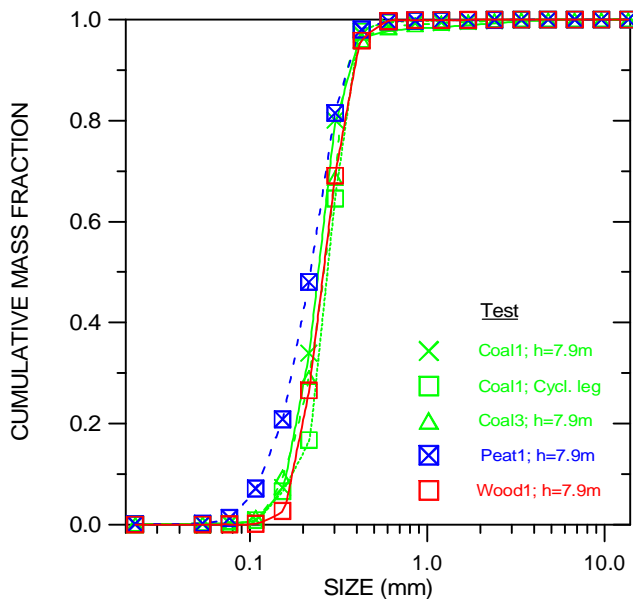


Fig. 2.4.1 Cumulative mass fractions of the inert fraction of samples taken from hole H11 (H=7.9 meter) and the cyclone leg during the tests with the various fuels. Input data: [Fig2_4_1.xls](#)

temperature of 850 °C in the bottom of the furnace, an excess air ratio of 1.2 corresponding to an oxygen concentration of 3.5% with coal as fuel and 3.2% with peat and wood measured on wet flue gases. The total amount of combustion air supplied was divided into primary air, 52-57%, and 34-36% was directed to the secondary air nozzles, while the remaining 8-12% was used to fluidize the ash classifier, particle seal and particle cooler (11,12 in Fig. 2.1.1). The load of the boiler gave a fluidizing velocity at the top of the combustion chamber between 5.7-6.0 m/s based on the total amount of air and the temperature at the top of the combustion chamber. The flue gas flow becomes 10% higher than the air flow as an effect of the combustion and moisture content in the fuel. By using the flue gas flow a fluidizing velocity of 6.2-6.5 m/s is obtained.

The bed material was pure silica sand with an average size of 0.32 mm according to the sieve curve given by the supplier of the bed material. In order to check this, the sieve curves in Fig. 2.4.1 of the inert fractions of five samples taken in the cyclone leg (11 in Fig. 2.1.1) and in hole H11 (h=7.9 meter) represent well the size distribution of the inert material circulating in the system. The average mass weighted sizes of these five samples are calculated to 0.34, 0.31, 0.33, 0.27 and 0.32 mm respectively. Results from five independent tests with operation at the reference case for longer continuous periods (more than 24 hours) are reported. Three of the tests were with bituminous coal and the two last tests with peat and wood chips. These tests are referred to as Coal1, Coal2, Coal3, Peat1 and Wood1. Between each of the tests Coal1, Coal2 and Coal3 more than 6 months passed, with complete turn down of the boiler in between, followed by a maintenance period and a new start-up. By comparing these three coal

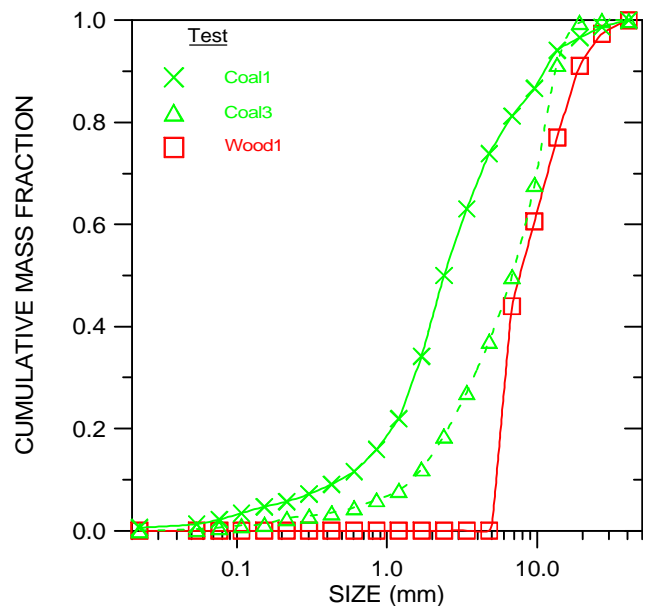


Fig. 2.5.1 Cumulative mass fractions of fuel samples taken from the belt weighters during the Coal1, Coal3 and Wood1 measurement. Input data: [Fig2_5_1.xls](#)

tests an idea of the reproducibility of the results can be obtained. The Coal3, Peat1 and Wood1 tests were carried out in conjunction with each-other, but after a shift of the bed material in order to avoid any possible influence of the fuel ash from one fuel affecting the test carried out later with another fuel. Apart from the five tests, two additional tests with bituminous coal are included for comparison of the oxygen concentration profiles in the combustion chamber. One of these tests denoted Precoal1 is reported in Åmand et al., 1991. The other one was carried out with lime addition in connection to test Coal2. This additional lime test is given the name Coallime1. Finally, an earlier test with wood chips (named Prewood1) is included for comparison of the solid samples taken from the combustion chamber during wood combustion. Results from this test is previously reported in Åmand & Leckner, 1993. Each of the tests Coal1 to Coal3, Peat1 and Wood1 is part of larger parameter studies reported elsewhere, Lyngfelt et al, 1995, 1996 and Åmand, 1996.

2.5 The Fuels

During the Coal1 test a low sulphur Colombian coal was used. In the Coal2 and Coal3 tests the coal was a Polish coal from the same ship load. The peat was taken from a field located 100 km from the city of Göteborg. The wood chips originated from pine and spruce and is a waste product from the wood and furniture industry, also in an area around Göteborg. In Table 2.5.1 analyses of fuel samples taken during each test period are given. The coals are high volatile, bituminous coals. Apart from the sulphur content the fuel analyses are very similar. Peat and especially wood chips contain much more volatiles and moisture than the bituminous coal. Especially

Table 2.5.1 Fuel characteristics

	Coal1	Coal2	Coal3	Peat1	Wood1
Particle size					
Mass mean (mm)	5.3	*	8.5	**	12.3
<1 mm (%)	15.9	*	6.1	0	0
Volatiles (wt% daf)	39.9	40.2	38.8	69.4	81.6
Proximate analysis (wt% a.r.)					
Combustibles	78.6	74.2	72.7	72.0	56.5
Ash	6.6	8.9	11.8	3.0	0.4
Moisture	14.8	16.9	15.5	25.0	43.1
Ultimate analysis (wt% daf)					
C	79.8	78.4	78.4	59.5	50.6
H	5.3	5.5	5.5	6.4	5.9
O	12.6	12.7	12.7	31.5	43.2
S	0.72	1.84	1.84	0.53	0.04
N	1.56	1.60	1.6	2.1	0.22
Heating value (MJ/kg low, daf)	31.8	31.09	31.09	22.33	18.73

* Similar to Coal3 ** Machined peat of a cylindrical form. Diameter 70mm; Length between 50 to 100 mm.

the higher volatile content leads to a different combustion behaviour of the fuels, influencing the oxygen concentration in the combustion chamber as well as the fuel loading.

Fig. 2.5.1 shows the result of sieving the fuel samples. The coal used during the Coal1 test contained more fines, (15.9 % compared to 6.1% less than 1 mm) which gives a somewhat lower mass weighted average size of 5.3 mm compared to 8.5 mm for the other coal. This small difference in size distribution and the similar fuel analyses make a comparison of the coal tests possible. The wood

chips used had a mass weighted average size of 12.3 mm with no pieces smaller than 5.6 mm. Peat was supplied as long cylinders with a diameter of 70 mm and a varying length of about 50 to 100 mm.

3 RESULTS

3.1 Mass- and Heat Balances

To get an idea of the accuracy of the measurements mass balances of fuel and air have been carried out. These data are then used in heat balances over the boiler and can be checked against the total amount of heat recovered by the water flowing through the boiler. Since no steam is generated in the boiler tubes, a temperature increase can be measured, making local heat balances over the various parts of the boiler possible.

3.1.1 Air- and Fuel Flows

The total amount of air supplied to the boiler was measured by a venturi nozzle located ahead of the fluidizing fan with proper lengths of the air channels both up- and downstream of the venturi. After the fluidizing fan the air is divided into primary air, secondary air and air to fluidize the ash classifier, particle seal and particle cooler. Each of these flows is measured individually, and by adding them a comparison with the total air flow becomes possible. Such a balance is shown in Table 3.1.1.1. The relative error in such a calculation is at most 6%. The air flows together with the flue gas flow recirculation flows are then used to calculate the fluidizing velocity through the bottom part of the combustion chamber and at the top of the furnace, Table 3.1.1.2. By calculating the stoichiometric air demand for each fuel, measuring the excess air ratio by determining

Table 3.1.1.1 Air flows

	Coal1	Coal2	Coal3	Peat1	Wood1
Total air flow to comb. chamber (kg/s)	3.65	3.54	3.54	3.68	3.67
Primary air flow (kg/s)	1.93	1.80	1.72	1.80	1.95
Total secondary air flow (kg/s)	1.25	1.24	1.29	1.34	1.33
Air to a classifier for bed material (kg/s)	0.15	0.15	0.19	0.15	0.20
Air to the particle seal	0.14	0.10	0.10	0.10	0.10
Air to the part cooler in the particle seal (kg/s)	0.11	0.05	0.15	0.16	0.00
Sum of flows excluding the total air flow (kg/s)	3.59	3.33	3.45	3.54	3.58
Error in air flow (kg/s)	0.06	0.22	0.10	0.13	0.08
Relative error in air flow (%)	1.8	6.1	2.7	3.6	2.2

Table 3.1.1.2 Fluidizing velocities						
	Coal1	Coal2	Coal3	Peat1	Wood1	
Superficial gas velocity						
in primary zone	4.12	3.81	3.85	3.71	3.43	
Superficial gas						
at the top based						
flue gas flow (m/s)	6.45	6.17	6.39	6.68	6.84	

Table 3.1.1.3 Fuel flows						
	Coal1	Coal2	Coal3	Peat1	Wood1	
Excess air ratio	1.21	1.21	1.21	1.21	1.23	
Stoichiometric air						
demand						
m ³ n/kg fuel burned	8.28	8.24	8.24	6.12	4.71	
Flow of oxygen to						
comb. chamb. m ³ n/s	0.62	0.60	0.60	0.62	0.61	
Fuel burned						
kg comb. burned/s	0.29	0.29	0.29	0.40	0.50	
Combustion efficiency	0.93	0.94	0.95	1.0	1.0	
Fuel flow based on						
air supply kg/s	0.40	0.41	0.42	0.56	0.88	
Fuel flow based on						
belt weighters kg/s	0.45	0.43	0.44	0.61	0.87	
Error in fuel flow (kg/s)	0.04	0.02	0.02	0.06	-0.01	
Relative error						
in fuel flow (%)	11	4	5	11	-1	

by determining the oxygen concentration in the flue gas, and then using the total amount of air supplied to the boiler, the amount of combustibles burned can be calculated, Table 3.1.1.3. By using the content of combustibles from Table 2.5.1 and the combustion efficiency, a fuel flow can be calculated and compared to the fuel flow measured by the belt weighters. A difference is then obtained with 10% higher fuel flow measured during the Coal2 and Coal3 tests. On the other hand less fuel was measured during wood combustion compared to the calculated value.

3.1.2 Ash Balances

In Table 3.1.2.1 the ash balances for the five tests are reported. Pneumatic senders from the secondary cyclone and the bag-house filter collect the ash. These senders stand on load cells making it possible to determine the weight of each batch of ash sent away to a large ash bin. Samples of this ash were collected and analysed on a Mac 400 instrument for

Table 3.1.2.1 Ash balances						
	Coal1	Coal2	Coal3	Peat1	Wood1	
Inert supplied with						
the fuel (kg/h)	96	98	128	66	13	
Inert out as ash in sec.						
cyclone ash (kg/h)	43	76	82	35	1	
Inert out as as in bag						
house filter ash (kg/h)	24	23	20	16	3	
Inert leaving the boiler						
as fly ash (kg/h)	66	99	103	50	4	
Difference in						
ash flow (kg/h)	30	-1	25	15	9	
Difference in ash flow						
relativ inert in fuel (%)	31	-1	20	23	70	

for combustibles, see Chapter 2.3. Based on the combustibles in these two flows the combustion efficiency can be calculated, Table 3.1.1.3, and the amount of inert is used in the ash balances in Table 3.1.2.1. With one exception the total amount of inert material leaving the boiler in the two ash flows never reached the amount supplied with the fuels. The reason for this difference could be that some ash left the combustion chamber as bottom ash despite the fact that the screw feeder for ash removal should have been closed during the tests. In the wood case

Table 3.1.3.1 Heat Balance (fuel)						
	Coal1	Coal2	Coal3	Peat1	Wood1	
Flow of combustibles						
with fuel (kg/s)	0.317	0.303	0.303	0.400	0.499	
Heating value of fuel,						
lower (kJ/kg)	31800	31090	31090	22326	18820	
Heat supplied with						
fuel (kW)	10095	9430	9418	8932	9392	
Moisture content of						
fuel (kg H ₂ O/kg fuel)	0.15	0.17	0.16	0.25	0.43	
Flow of moisture (kg/s)	0.060	0.069	0.065	0.139	0.381	
Heat loss moisture (kW)	149	172	161	347	952	
Heat loss radiation (kW)	202	189	188	179	188	
Heat loss flue gas (kW)	441	459	449	568	663	
Heating value of char						
lower (kJ/kg)	33000	33000	33000	33000	33000	
Heat loss due to char						
in fly ash (kW)	742	579	522	15	4	
Difference (kW)	8561	8031	8097	7823	7585	

fact that the screw feeder for ash removal should have been closed during the tests. In the wood case the calculation becomes uncertain because of the low total flow of ash in this case.

3.1.3 Heat Balances

In Table 3.1.3.1 the heat balances related to the fuel supply are given. Apart from the amount of heat supplied with the fuel, all heat losses are calculated and specified in Table 3.1.3.1. This gives the possibility to calculate the net heat supply to the boiler, an amount that should be equal to the heat recovered by the water passing through the whole boiler. Two different values of this amount are calculated, Table 3.1.3.2, based on two independent measurements of the flow of boiler water through the combustor. In Table 3.1.3.2 the heat balances over the various parts of the combustor are reported. The different parts are: furnace, cyclone, convection pass, ash classifier, particle cooler and economiser. The sum of heat recovered in these parts should be equal to the independent calculation of the total amount of heat recovered using the higher flow of water through the boiler. A comparison of these values show an excellent agreement for all the five tests. If the lower flow of water is used in each calculation of the amount of heat recovered in a comparison of the net supply of heat on the fuel side

Table 3.1.3.2 Heat Balance (water)					
	Coal1	Coal2	Coal3	Peat1	Wood1
H2O flow1 boiler (kg/s)	40.8	39.5	39.0	38.7	39.6
H2O flow2 boiler (kg/s)	42.8	42.8	42.8	42.7	43.9
Total amount of heat recov. by H2O flow1 (kW)	8157	7752	7953	8079	7507
Total amount of heat recov. by H2O flow2 (kW)	8527	8348	8654	8832	8232
Q, furnace (kW)	3175	3561	3428	3681	3235
Q, cyclone (kW)	494	500	459	478	491
Q, conv. pass (kW)	2931	3130	3151	3567	3652
Q, economizer (kW)	536	599	776	837	829
Q, classifier (kW)	182	185	141	154	19
Q, particle cooler (kW)	1215	376	703	119	9
Q, total by addition (kW)	8532	8350	8658	8836	8235
Q, net by fuel (kW)	8561	8031	8097	7823	7585
Q, net fuel-Q, H2O flow1	404	279	144	-256	78
Relative difference (%)	5	4	2	-3	1

the balance closes within $\pm 5\%$. This means that there is a good control of the accuracy of the air and fuel flows.

3.2 Characterisation of the Gas Phase

3.2.1 Oxygen Profiles during Coal Combustion

The measured oxygen concentrations on the centre line of the combustion chamber during coal combustion are shown in Fig. 3.2.1.1. A general shape can be recognised in all profiles. Fairly low oxygen concentrations are measured close to the bottom plate. A falling tendency is then seen up to the level where secondary air is introduced and then there is a gradual increase of oxygen towards the exit of the combustion chamber. The reason for this typical shape of the oxygen profile on the centre line becomes evident when looking at Fig. 3.2.1.2. In addition to the centre-line profiles, profiles closer to the front and back walls (the fc- and bc positions in Fig. 2.1.1.1) are plotted in Fig. 3.2.1.2 for comparison. The fc- and bc positions are located closer to the walls from where the secondary air is entering, and therefore a clear increase of the oxygen concentration is recorded at the height of secondary air injection. From about 3 meter the slow increase of oxygen along the centre-line is followed by a decrease in the oxygen concentration along the front and back sides of the combustion chamber. In

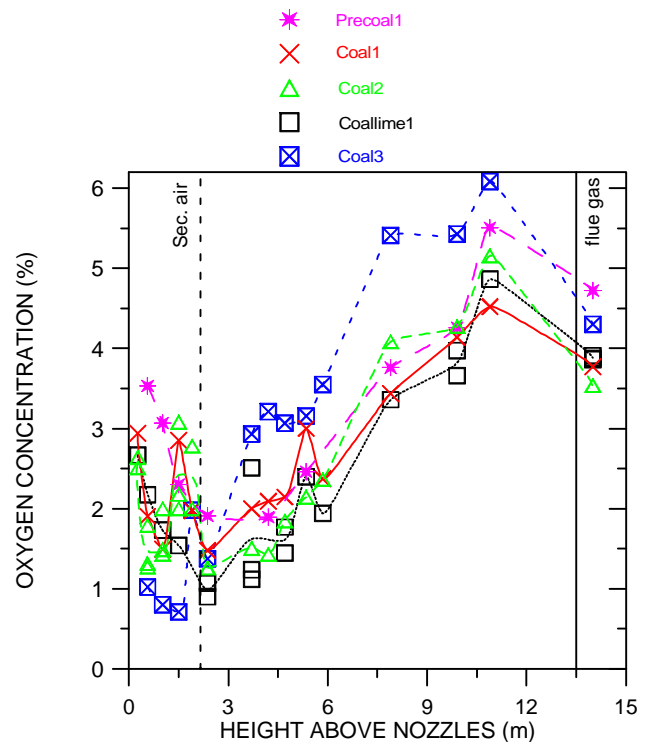


Fig. 3.2.1.1 Vertical profiles of oxygen along the centre line of the combustion chamber for the different test series with bituminous coal as fuel. Input data: [Fig321_1.xls](#)

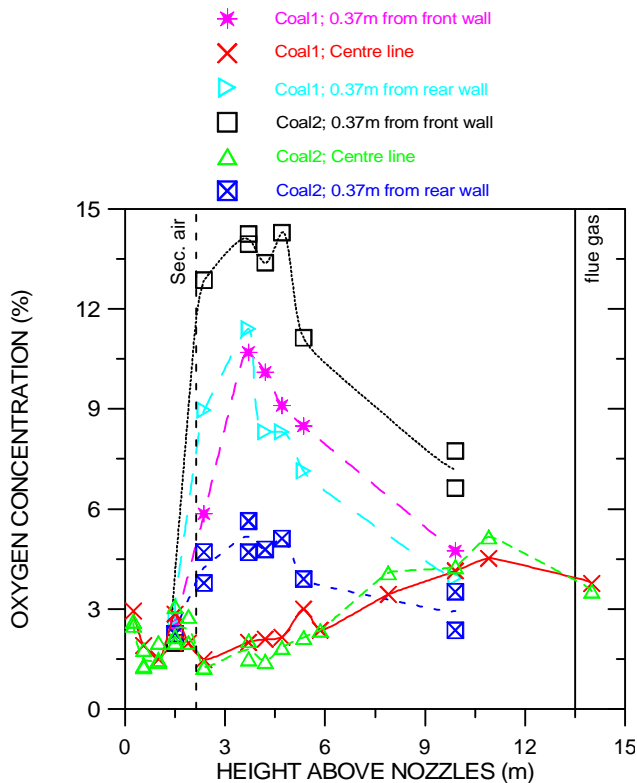


Fig. 3.2.1.2 Vertical profiles of oxygen in the combustion chamber during the Coal1 and Coal3 tests. Input data: [Fig321_2.xls](#)

Fig. 3.2.1.2 data from the Coal1 and Coal2 tests are given. Even in these two tests, when the boiler was operated very similarly, a difference in the oxygen concentrations were obtained at the front and back sides of the combustion chamber. During the Coal2 test a much lower oxygen concentration is noticed along the back wall compared to the situation during the Coal1 test. This difference is interpreted as an effect of partial plugging of two or more of the nozzles located at the back wall of the combustion chamber, Fig. 2.1.1.1.

In order to get an even better picture of the oxygen concentrations over the whole cross-section, measurements in nine positions at two heights (3.7 and 9.9 meter) were performed during the Coal2 test, Fig. 3.2.1.3. In this figure a complicated picture shows up. In the front positions, the high oxygen concentration at the fc position is not seen for either the fr- or fl positions. One plausible explanation for this could be partial plugging of secondary air nozzles again. At the rear positions an opposite result was obtained, much higher oxygen concentrations in the br- and bl positions compared to the bc position. In this case the influence of the fluidizing air to the particle seal and ash classifier, see chapter 2.1.1, have some influence, but this needs additional tests for verification. As input for combustion modelling the data can be treated as follows:

The nine-position measurement at 3.7 and 9.9 meter verified that the three-position measurements (fc, cc

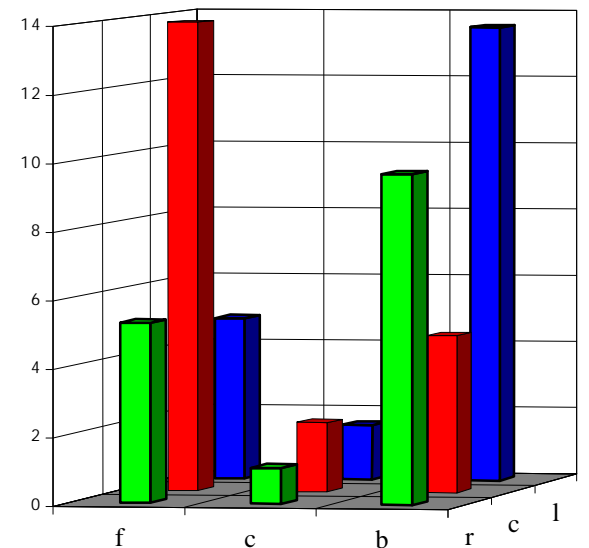
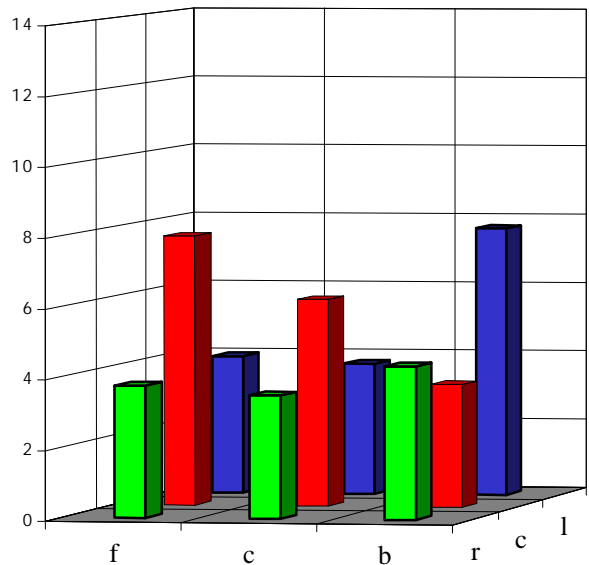


Fig. 3.2.1.3 Oxygen concentration (%) in furnace cross-section at 9.9 meter (top) and 3.7 meter height (bottom) during the Coal2 test. Input data: [Fig321_3.xls](#)

and bc) gave a reasonable representation of the cross-section average and were used to improve the accuracy of the data. Thus, the cross-sectional averages were obtained from the three-position measurements, after a correction derived from the nine-position measurement data. Below the secondary air inlets, the values measured in the cc position were used as cross-section averages, since there is no significant variation in the time-average concentration over the cross-section. This procedure for data processing is identical with that used by Lyngfelt et al., 1996.

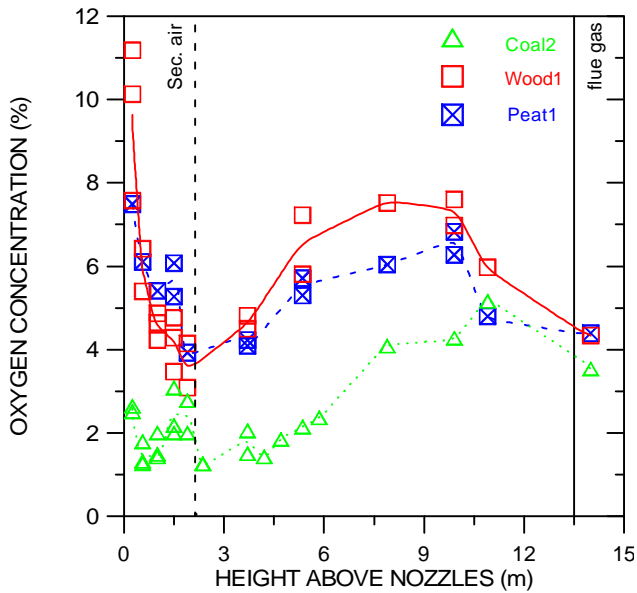


Fig. 3.2.2.1 Vertical profiles of oxygen along the centre line in the combustion chamber for the tests Coal2, Peat1 and Wood1. Input data: [Fig322_1.xls](#)

3.3.2 Oxygen Profiles during Peat and Wood Combustion

The switch from coal to high volatile fuels, such as peat and wood, without changing the operating parameters, changes the oxygen profiles in the combustion chamber due to different combustion behaviour. This becomes clear from Figs. 3.2.2.1 to 3.2.2.3. In Fig. 3.2.2.1 the oxygen profiles on the centre-line for the three fuels are compared. Much higher oxygen concentrations were measured for peat and wood compared to coal. The difference is largest below the secondary air inlet, where much more char is burning in the coal case compared to peat and wood. Above the secondary air inlet the profiles have a similar character (also seen in Fig.3.2.1.1 for the coal runs) determined by the insufficient penetration depth of secondary air. At a height of 10.8 meter where the combustion gases are pulled over towards the cyclone, as well as in the cyclone, the oxygen concentrations in the different cases become more similar. This means that, if compared to the oxygen level at the 9.9 meter

position, much more combustion takes place near the cyclone and in the cyclone in the peat and wood cases compared to coal. This can be explained by the improved mixing between unburned combustible matter and oxygen.

Another picture of the different combustion behaviour of the three fuels is given by the results from the nine point measurement carried out at four heights during the Wood1 and Peat1 tests, Figs. 3.2.2.2 to 3.2.2.3. At the lowest level (1.5 meter), located below the secondary air inlet, a non-uniform oxygen concentration was obtained for both fuels. This indicates that other factors may be of importance than the incomplete secondary air penetration discussed earlier. One example is the higher oxygen concentration along the left wall which can be recognised for both fuels. Out of these three positions only the bl position in the corner can be explained by the fact that the fluidizing air of the return leg is re-entering into the combustion chamber in this corner. Nevertheless, in order to understand the variations over the cross-section more measurements focusing on this issue are needed.

Comparing the nine point measurement at 3.7, 5.4 and 9.9 meter of the peat and wood chips test, large similarities are observed. Both cases show less oxygen closer to the front wall than at the back wall, (with exception of the fc-position). These lower oxygen concentrations closer to the front are different from the coal case and are explained as an effect of the higher volatile content of peat and wood, volatiles which are released to a greater extent at the front wall where the fuel is supplied, Fig. 2.1.1. This conclusion is supported by the fact that the concentration of reducing species, such as carbon monoxide, hydrocarbons and ammonia show an opposite trend with much higher concentrations at the front wall compared to the centre and back positions.

When only centre-line measurements were available, the accuracy was enhanced by comparing with cross-sectional averages from nine-position measurements at 3.7, 5.4 and 9.9.

Below the secondary air inlets, the values measured in the cc position were not corrected, since the variation over the cross-section at 1.5 meter is much less below the secondary air level at 2.2 meter.

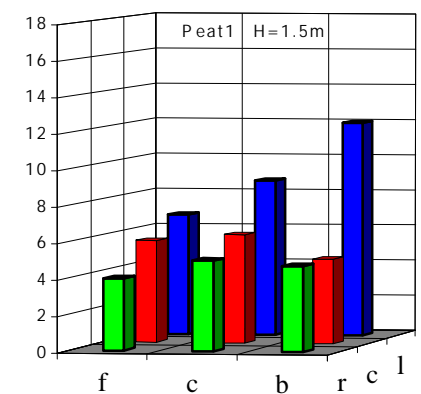
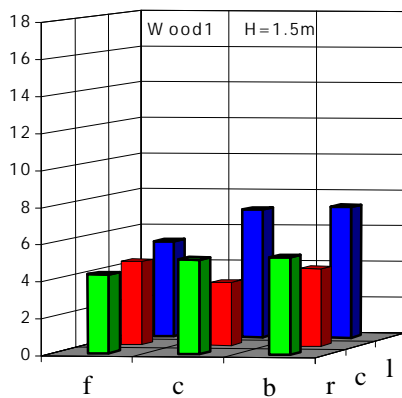
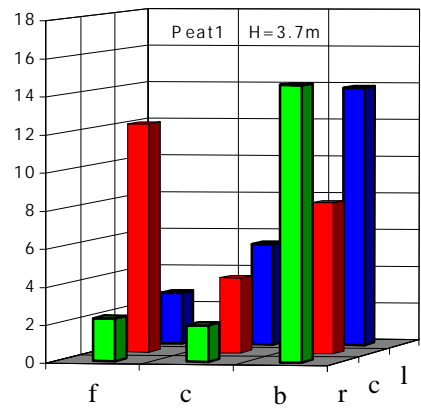
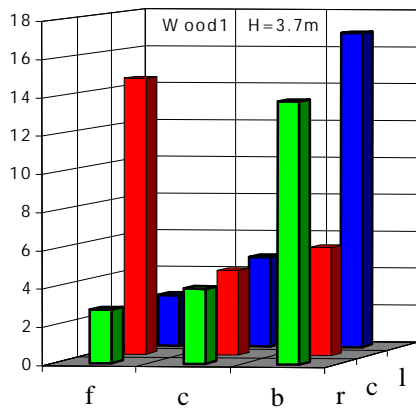
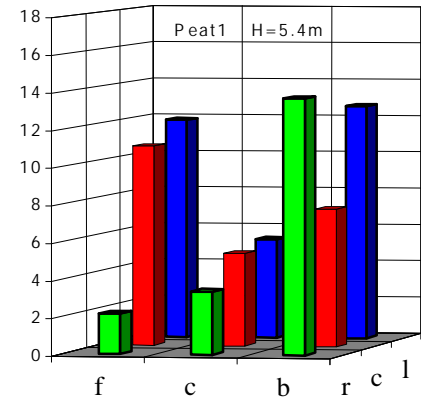
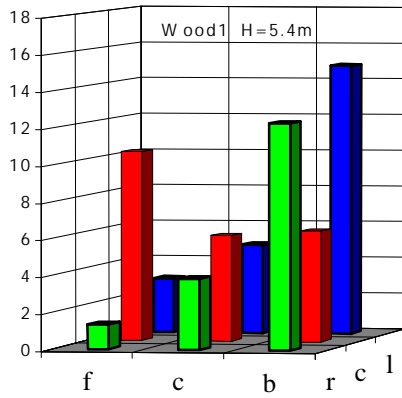
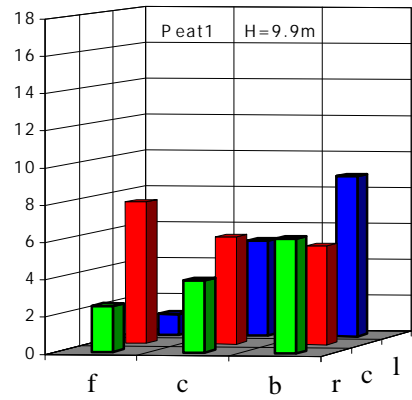
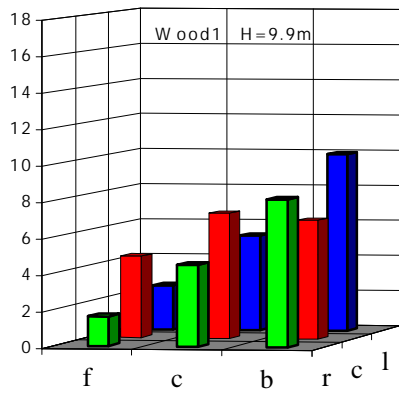


Fig. 3.2.2.2 Oxygen concentration (%) in furnace cross-section at 1.5, 3.7, 5.4 and 9.9 meter during the Wood1 test. Input data: [Fig322_2.xls](#)

Fig. 3.2.2.3 Oxygen concentration (%) in furnace cross-section at 1.5, 3.7, 5.4 and 9.9 meter during the Peat1 test. Input data: [Fig322_3.xls](#)

3.3 Characterisation of the Particle Phase

The particle phase is characterised by: the vertical solids concentration profile, the char content in the solid samples taken in the combustion chamber, the average size of the inert- and the char-fractions of these solids samples, and finally, a calculation of the char content (both mass and area) in the combustion chamber. This characterisation is first demonstrated for the three coal cases and thereafter applied to the Peat1 and Wood1 tests.

3.3.1 Solids Concentration Profiles during Coal Combustion

The vertical cross-section average density profile is determined by pressure drop measurements. The representation of the profiles follows the procedure of Johnsson & Leckner (1995). The vertical solids concentration profile is divided into three zones: a dense bottom bed, a splash zone, and a transport zone. The bottom bed is identified by a constant pressure drop, which leads to a constant time and cross-sectional average particle concentration (σ) up to a height of H_x (the bottom bed height) provided that acceleration effects can be neglected. The following expressions represent the vertical solids concentration profile (according to Johnsson & Leckner 1995):

For $h < H_x$

$$\sigma = \sigma_x$$

and for $H_x < h < H_{exit}$

$$\sigma = (\sigma_x - \sigma_{2,H_x}) \exp(-a(h - H_x)) + \sigma_{2,H_x} \exp(K(H_{exit} - h))$$

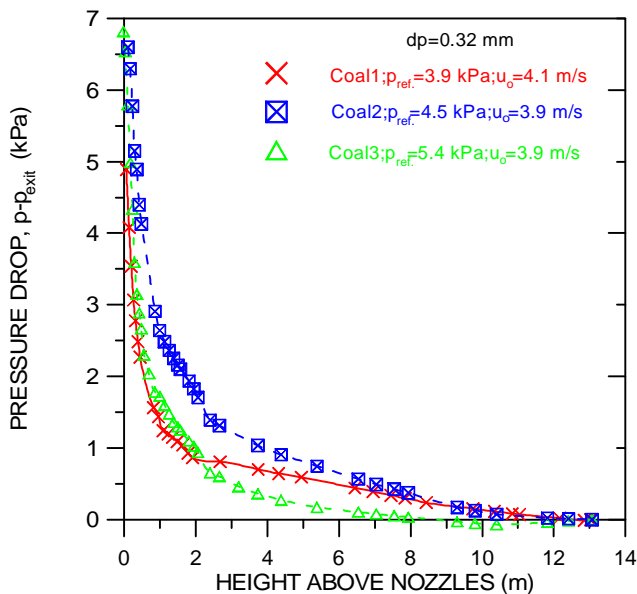


Fig. 3.3.1.1 Vertical pressure drop profiles in the combustion chamber for the three coal tests. Input data: [Fig331_1.xls](#)

where the solids concentration at the upper position of the bottom bed due to dispersed solids, σ_{2,H_x} , is

$$\sigma_{2,H_x} = \sigma_{exit} \exp(K(H_{exit} - H_x))$$

σ_{exit} and H_{exit} are the particle density and height at the exit of the combustor, a and K are decay constants fitted to give a good correlation to measured values.

Fig. 3.3.1.1 shows the vertical pressure drop profiles for the Coal1 to Coal3 tests. Two important parameters for the distribution of solids are given in the figure, that is, the superficial gas velocity of the bottom bed (u_o) and the reference pressure drop between a pressure tap just above the air distributor and a tap located 1.7 meter above the air distributor, the reference pressure drop (p_{ref}).

Apart from these two parameters the type and size of the bed material are also important. In all three cases the bed material was silica sand with an average size of 0.32 mm (mass weighted). The particle density of silica sand is 2600 kg/m³. This yields a terminal velocity (u_t) of 2.1 m/s.

A comparison of u_o and p_{ref} for the three coal runs shows that p_{ref} varies between 3.9 kPa and 5.5 kPa. For the Coal2 and Coal3 tests the total pressure drop across the whole combustion chamber was kept constant, although the p_{ref} values differ between 4.5 kPa and 5.5 kPa. This can be seen in Fig. 3.3.1.1 and it was also confirmed by a single pressure transducer used for supervision and control of the boiler operation. Since the pressure drop is proportional to the solids concentration, slightly different concentrations are obtained in Fig. 3.3.1.2 for the Coal2 and Coal3 tests. A slightly higher

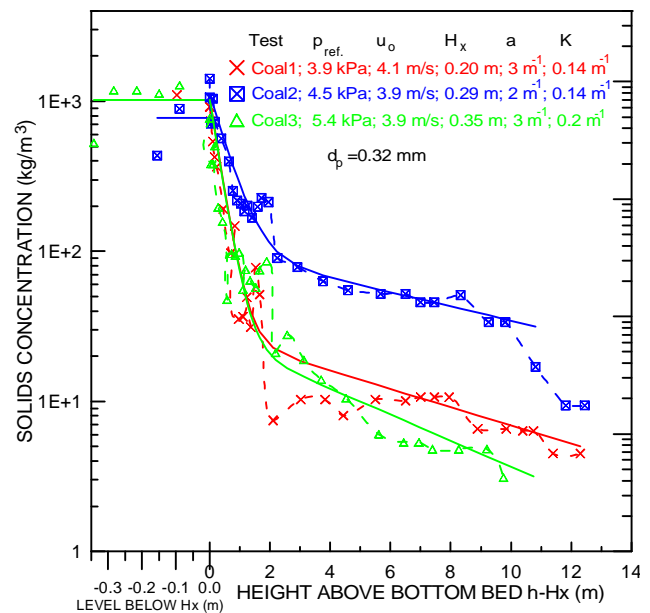


Fig. 3.3.1.2 Vertical profiles of solids concentration as obtained from data of Fig. 3.3.1.1. (Note the change in the horizontal scale). Input data: [Fig331_2.xls](#)

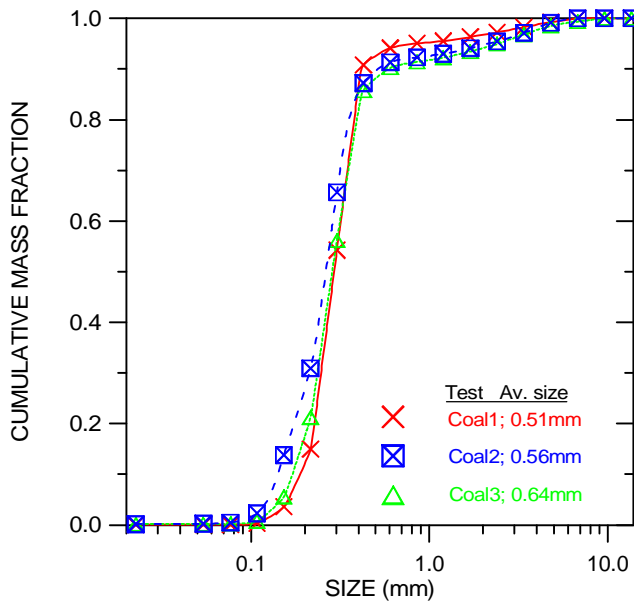


Fig. 3.3.1.3 Cumulative mass fractions of the sample taken from hole H2 (H=0.56 meter) in the combustion chamber during the Coal1 to Coal3 tests. Input data: [Fig331_3.xls](#)

bottom bed but lower top density is seen in Fig. 3.3.1.2 in the Coal3 test compared the Coal2 test. The reason for these differences could be related to the difference in size of the bed material, Fig. 3.3.1.3. The mass weighted average particle size of the bed sample taken from position H2 (H=0.56 meter above the air distributor) is larger during the Coal3 measurement compared to the two other occasions. This is probably caused by different efficiency in the operation of the ash classifier. Nevertheless, the different pressure profiles in Fig. 3.3.1.1 influence the evaluation of the solids concentration profile and the fitting of the decay constant "a" as can be seen in Fig. 3.3.1.2. For this reason all three profiles are used together with the char samples to determine the char content in the combustion chamber.

3.3.2 Char Content in Solid Samples during Coal Combustion

Fig. 3.3.2.1 shows the char content in all samples taken in the combustion chamber and cyclone leg during the three measurements with coal. Most of the samples were taken in the splash zone (h=0.56 meter) and cyclone leg. There is some scatter in the results but despite the scatter a clear dependence of the char content on the height in the combustion chamber can be seen, expressed as a straight line in Fig. 3.3.2.1. The cyclone leg samples are included in this fitting of the results by regarding these data to be representative for the conditions at the exit of the combustion chamber at h=12 meter. In one of the cyclone leg samples a char concentration of 4.8% was obtained. This deviating sample is omitted in the evaluation.

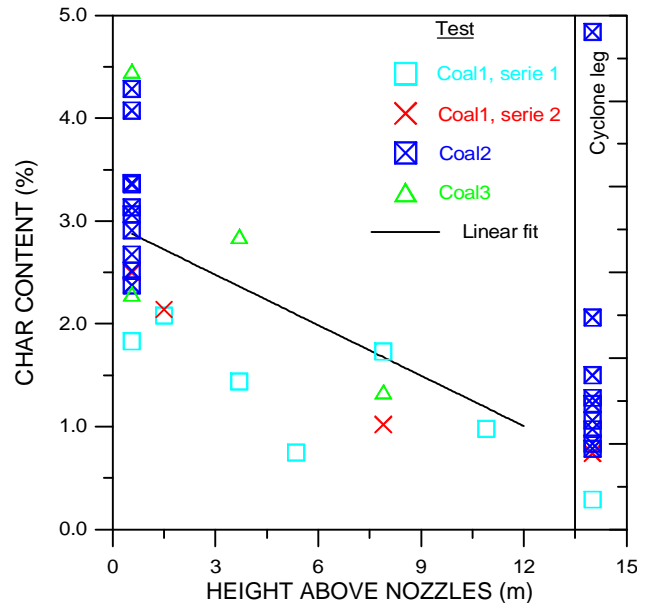


Fig. 3.3.2.1 Char concentration in solid samples taken in the combustion chamber during the Coal1 and Coal3 tests. Input data: [Fig332_1.xls](#)

3.3.3 Average Size of the Char Fraction of the Bed Material during Coal Combustion

Some of the samples from Fig. 3.3.2.1 have been sieved. This procedure made an analysis of the char content in each fraction possible which results in sieve curves like Fig. 3.3.3.1 and Fig. 3.3.3.2. The two samples were taken during different tests. The total char concentration differs between these two samples with a factor of two but the size distributions are almost identical. The advantage of representing the data as in Fig. 3.3.3.1 and Fig. 3.3.3.2 lies in the

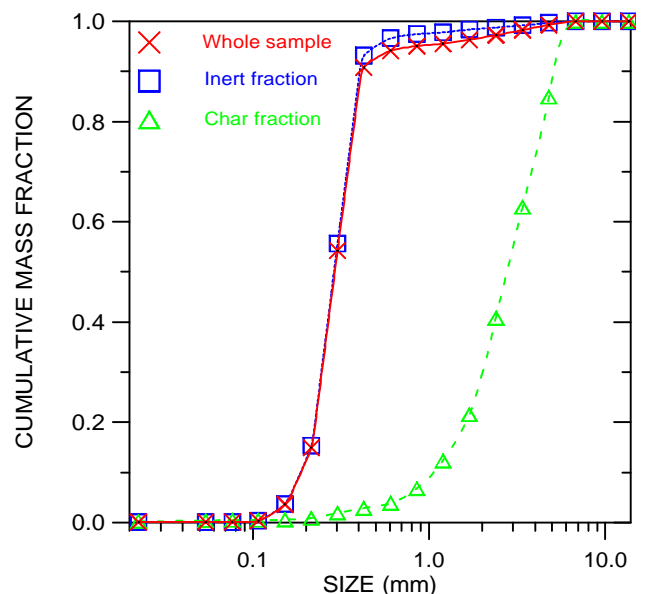


Fig. 3.3.3.1 Cumulative mass fractions of the whole sample, the char fraction and the inert fraction. Sample taken during the Coal1 test from hole H2 (H=0.56 meter) in the combustion chamber. Input data: [Fig333_1.xls](#)

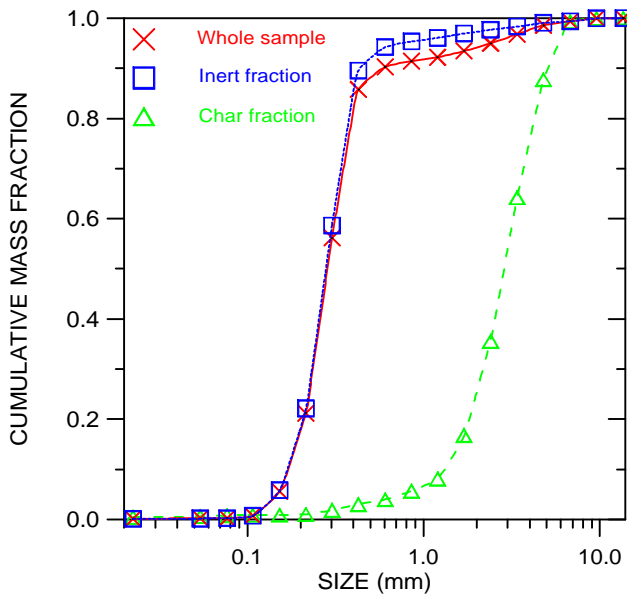


Fig. 3.3.3.2 Cumulative mass fractions of the whole sample, the char fraction and the inert fraction. Sample taken during the Coal3 test from hole H2 (H= 0.56 meter) in the combustion chamber. Input data: [Fig333_2.xls](#)

possibility to calculate the average size of the whole sample, the char fraction and the inert fraction. This calculation gives both the mass weighted and the surface weighted mean particle diameter as function of the height in the combustion chamber. This has been carried out for all the samples plotted as cross and squares in Fig. 3.3.2.1. The result for the char fraction is shown in Fig. 3.3.3.3. Again a good similarity is seen between the samples taken at the two different occasions at the same position in the combustion chamber. As before, the particle diameter of the cyclone leg samples is used in the fitting of linear expressions of the relationship between mean diameter and height in the combustion chamber. Similar curves as in Fig. 3.3.3.3 for the whole sample and inert fraction have also been evaluated.

3.3.4 Char Content in the Combustion Chamber during Coal Combustion

The vertical solids concentration profiles given in Fig. 3.3.1.2 and the linear fit of the char content in the combustion chamber (Fig. 3.3.2.1) yield the mass of char in the combustion chamber as function of height, assuming the sample to be representative for the combustion chamber cross-section. By numerical integration and normalisation to the total amount of char, the curves in Fig. 3.3.4.1 are obtained. The vertical solids concentration has a dominant influence on the shape of the curves. This means that the difference in the exponential expressions in Fig. 3.3.1.2 is repeated as a difference in the cumulative char content. Despite this difference the solid lines in Fig. 3.3.4.1 show that more than 80% of

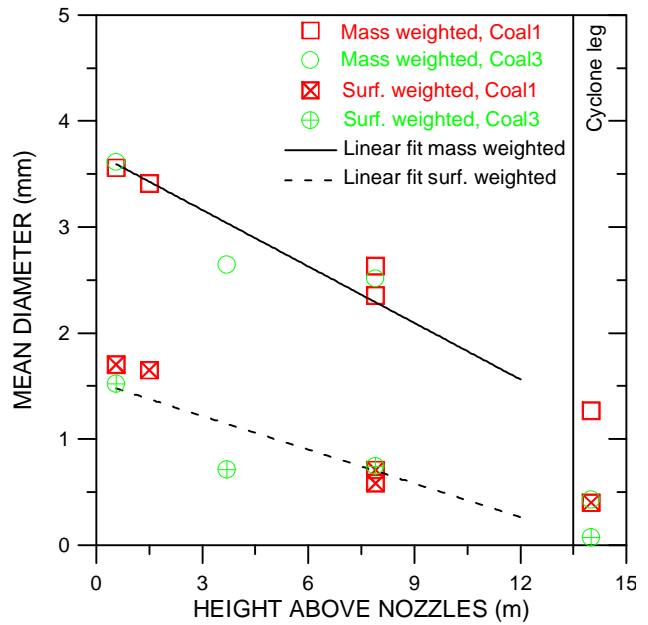


Fig. 3.3.3.3 Mass and surface weighted mean diameter for the char fraction of samples taken in the combustion chamber during the Coal1 and Coal3 tests. Input data: [Fig333_3.xls](#)

of the mass of char is retained in the bottom bed and splash zone (below 2 meter). If one looks at the external surface of the char and not at the mass of char, similar calculations are possible using the linear fit of the surface weighted mean particle diameter of Fig. 3.3.3.3. This gives the curves in Fig. 3.3.4.2. Also in these calculations the results are a consequence of the vertical solids concentration profile, but the values become somewhat lower with 70 % of the total external char surface found below the 2 meters level.

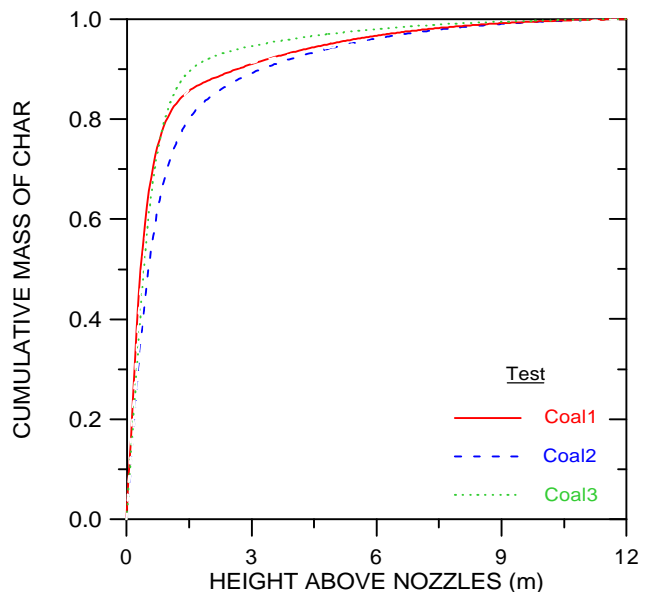


Fig. 3.3.4.1 Cumulative mass of char in the combustion chamber as function of height for the tests: Coal1, Coal2 and Coal3. Input data: [Fig334_1.xls](#)

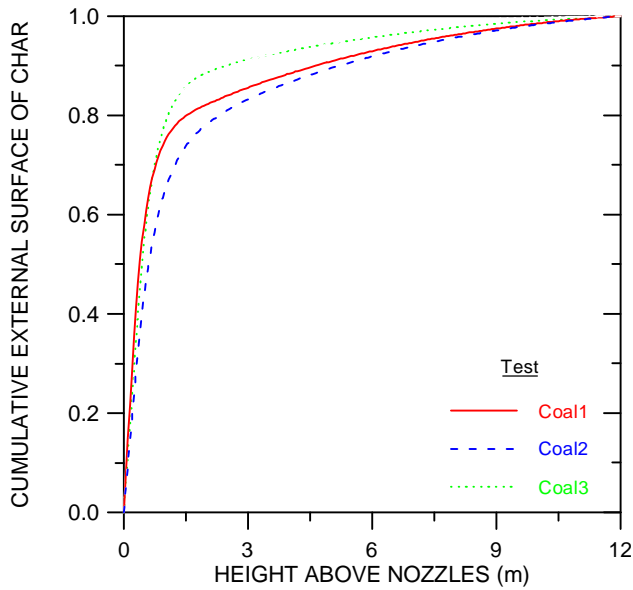


Fig. 3.3.4.2 Cumulative external surface of char in the combustion chamber as function of height for the tests: Coal1, Coal2 and Coal3. Input data: [Fig334_2.xls](#)

3.3.5 Solids Concentration Profiles during Peat and Wood Combustion

Fig. 3.3.5.1 shows the vertical pressure drop profiles for the three tests Coal3, Peat1 and Wood1. These three tests were run after each other and very similar pressure drop profiles were achieved. This leads to almost the same bottom bed height and identical values of the decay constants when using the evaluation procedure described in Chapter 3.3.1. The Coal3 test is therefore used as reference when the char contents for peat and wood are to be compared.

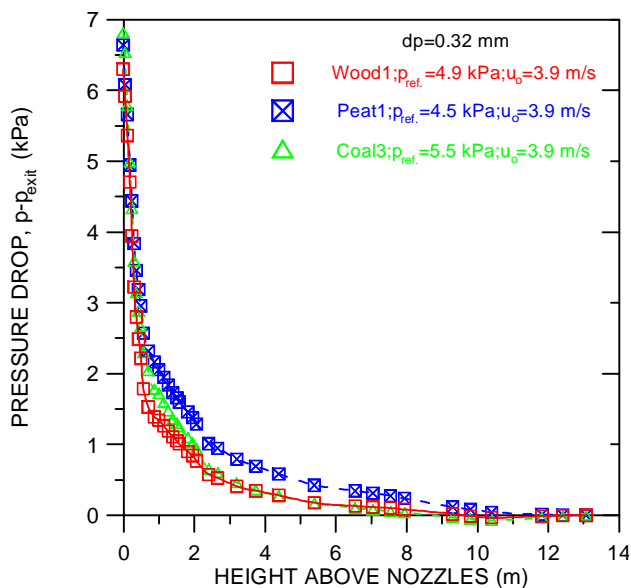


Fig. 3.3.5.1 Vertical pressure drop profiles in the combustion chamber for the tests Coal3, Peat1 and Wood 1 tests. Input data: [Fig335_1.xls](#)

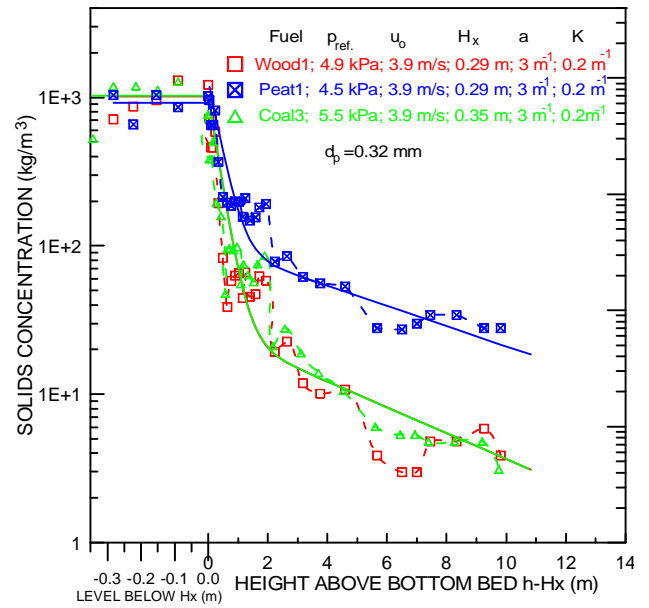


Fig. 3.3.5.2 Vertical profiles of solids concentration as obtained from data of Fig. 3.3.5.1. (Note the change in the horizontal scale) Input data: [Fig335_2.xls](#)

3.3.6 Char Content in Solid Samples during Peat and Wood Combustion

One can expect that the high volatile fuels, peat and wood, result in much less char to be left in the solid phase for combustion compared to coal. This assumption is confirmed in Fig. 3.3.6.1. For comparison the "straight" line for coal taken from Fig. 3.3.2.1 is inserted into Fig. 3.3.6.1. For peat the char concentration in the samples is about one tenth of what was obtained for coal. Wood chips gave even

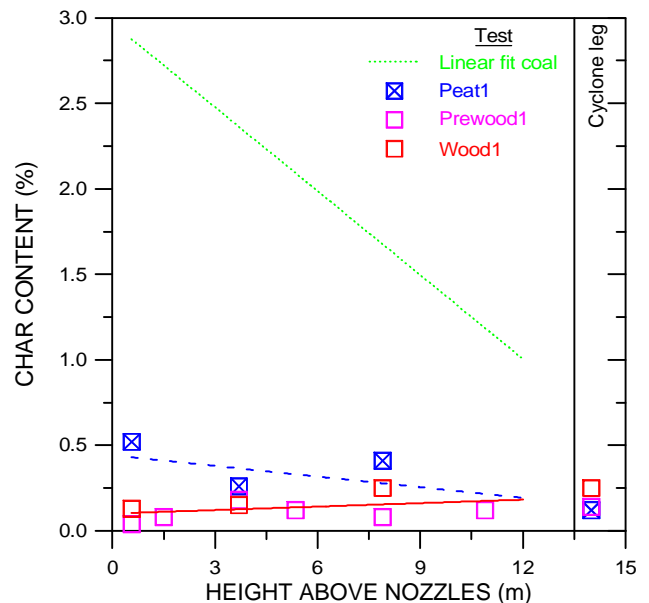


Fig. 3.3.6.1 Comparison of the char concentrations in solid samples taken in the combustion chamber during the tests: Peat1, Wood1 and Prewood1. Dotted line adopted from Fig. 3.3.2.1. Input data: [Fig336_1.xls](#)

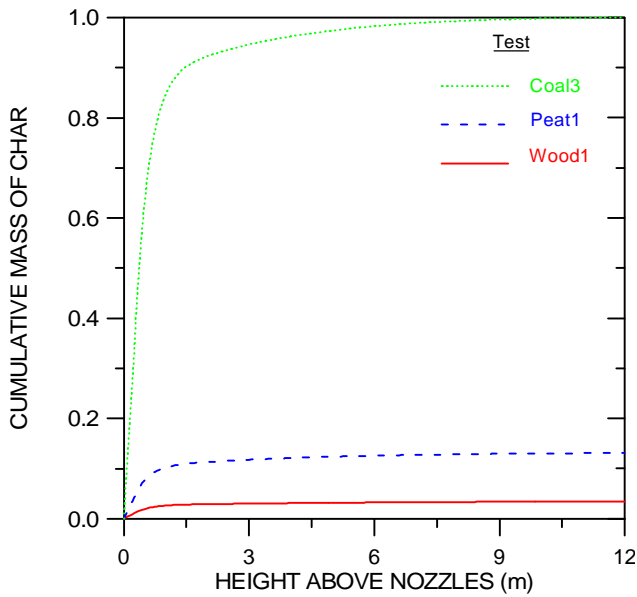


Fig. 3.3.7.1 Cumulative mass of char in the combustion chamber as function of height for the tests: Coal3, Peat1 and Wood1. Data for Peat1 and Wood1 normalised to the amount obtained for the Coal3 test. Input data: [Fig337_1.xls](#)

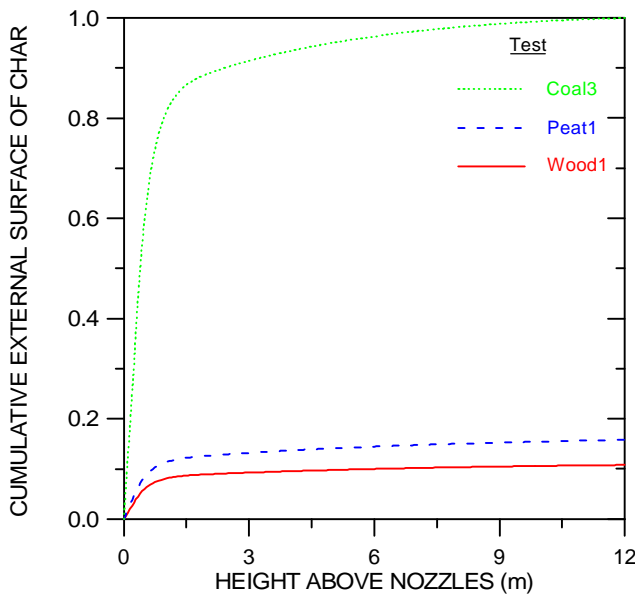


Fig. 3.3.7.2 Cumulative external surface of char in the combustion chamber as function of height for the tests: Coal3, Peat1 and Wood1. Data for Peat1 and Wood1 normalised to the amount obtained for the Coal3 test. Input data: [Fig337_2.xls](#)

lower char concentrations, about half of the values achieved for peat. The values for wood increase from about 0.1% char in the sample taken close to the bottom to 0.2% in the sample taken at the top of the combustion chamber. This means that the char concentrations in the solid samples taken during wood combustion show an opposite trend as function of height in the combustion chamber compared to what is measured for peat and coal.

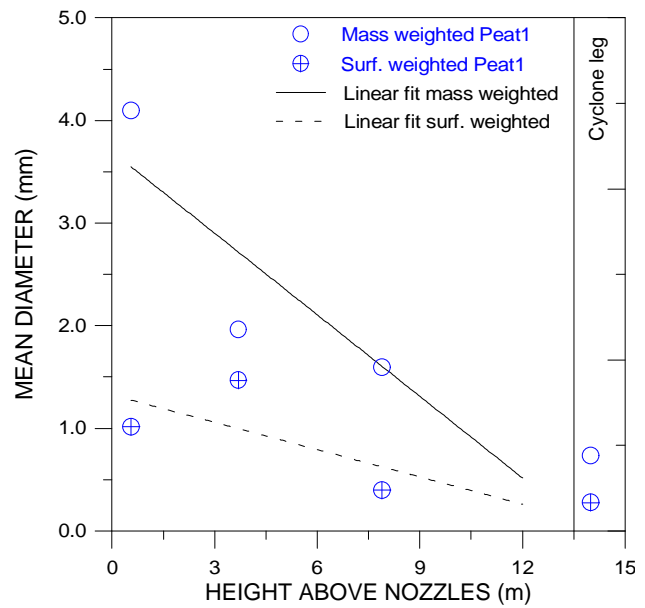


Fig. 3.3.7.3 Mass and surface weighted diameter for the char fraction of samples taken in the combustion chamber during the Peat1 test. Input data: [Fig337_3.xls](#)

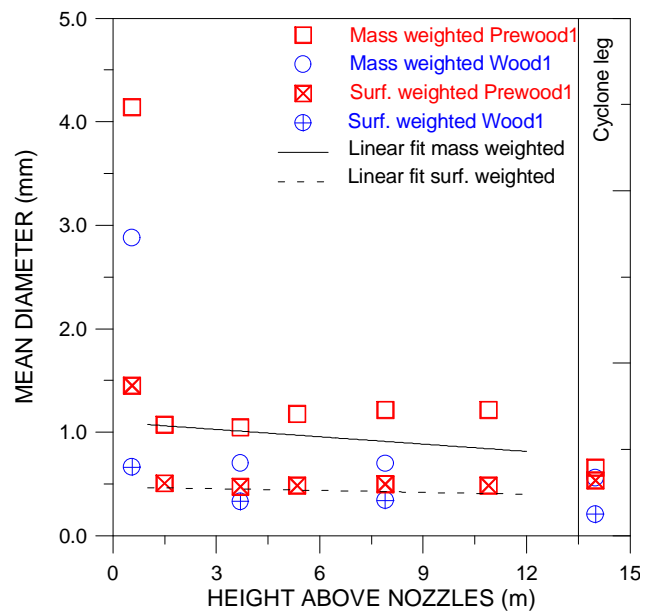


Fig. 3.3.7.4 Mass and surface weighted diameter for the char fraction of samples taken in the combustion chamber during the Prewood1 and Wood1 tests. Input data: [Fig337_4.xls](#)

3.3.7 Char Content in the Combustion Chamber during Peat and Wood Combustion

The vertical solids concentration profiles in Fig. 3.3.5.1 together with the linear fit of the char content in the solid samples taken in the combustion chamber, Fig. 3.3.6.1, yields the mass of char in the combustion chamber as function of height. By numerical integration and normalisation to the total amount of char in the Coal3 case, the curves in Fig.

3.3.7.1 can be plotted. Compared to the coal case as a reference the char content in the combustion chamber during peat combustion is only 13.5%. Wood combustion results in even less char, only 3.5% of the coal value. In all three cases more than 80% of the mass of char is retained in the bottom bed and splash zone (below 2 meter). Related to the external surface area of the char, a somewhat different picture is obtained, Fig. 3.3.7.2: for peat a slightly higher external char surface area (15.8%) is calculated. The reason is that the char in the peat case is found in particles of slightly smaller average sizes (surface weighted), Fig. 3.3.7.3 compared to coal, Fig. 3.3.3.3. The importance of the surface weighted average sizes on the total external surface areas becomes even more evident in the wood case. During wood combustion the surface weighted average sizes in the solid samples taken was, with one exception (position H2, H=0.65m), below 0.5 mm, Fig. 3.3.7.4. This difference in average size increases the amount of char based on the external area to 10.8% compared to the value of only 3.5% if the comparison is based on the mass of char.

4 DISCUSSION

4.1 Oxygen Concentration Profiles

The reasons for the typical shape of the oxygen concentration profiles in the Chalmers boiler shown in Figs. 3.2.1.1-3.2.1.2 have only been partly explained. The insufficient penetration depth of the secondary air in combination with partial plugging of some of the secondary air nozzles can explain the profiles at the levels which are higher than the injection level of 2.2 meter. By comparing the

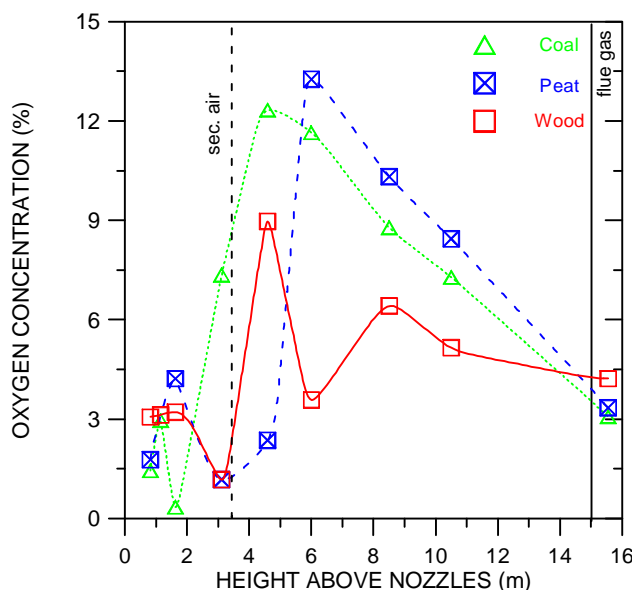


Fig. 4.1.1 Vertical cross-section averaged profiles of oxygen in the combustion chamber of a lab-scale CFB burning coal, peat and wood. Input data: [Fig4_1_1.xls](#)

Chalmers data with tests performed in a lab-scale facility, Knöbig et al., 1997, an interesting picture shows up, Fig. 4.1.1. Due to the slim and tall geometry of the lab-scale facility (inner diameter=0.1m; height=16m) no problems with secondary air penetration were present in Fig. 4.1.1, where the oxygen concentration profiles measured across the cross-section area increase above the secondary air injection level for all the three fuels tested.

The low oxygen concentrations in the bottom part of the Chalmers boiler (1-3%) during coal combustion needs some further comments. If these low oxygen concentrations present, even after corrections for the staging of the air supply, are supposed to represent the oxygen concentrations in the entire flow of air/flue gas passing through the bottom part of the combustion chamber, large errors will be introduced in the calculation of the local fuel consumption, Lyngfelt et al., 1996. The key to this conclusion is the data deduced from the fuel distribution curves, Figs. 3.3.4.1-3.3.4.2. The gas concentration measurements indicate that 71% of the combustion and 94% of the fuel conversion (to CO₂, CO and hydrocarbons) take place below 0.26 meter, Lyngfelt et al., 1996. This is unlikely, considering that only 26% of the solid combustible mass is found below this level, Fig. 3.3.4.1 and 24% of the combustible surface area, Fig. 3.3.4.2. The reason for this discrepancy is a bypass flow (or through-flow) of gas with a high oxygen content assumed to be made up of bubble chains or channels creating short circuits of gas bypassing the bottom bed with a much higher velocity than the remaining gas flow. These large velocity differences result in a poor representation of oxygen concentration of the flow measured by the gas extraction probe. However, by assuming a considerable bypass of air, an average oxygen concentration of the flow of 11.3% was calculated at a height of 0.26 meter above the bottom plate, Lyngfelt et al., 1996. This value should be compared to the measured oxygen concentration at this level of only 2.5 %, Fig. 3.2.2.1. The value of 11.3% oxygen in the gas flow, yields a reasonable agreement between data for the progress of fuel conversion based on either the solids or the gas concentrations. The conclusion is that interpretation of gas concentrations measured by a gas extraction probe in the lower part of the combustion chamber of a CFB boiler is difficult, because of a considerable bypass flow accompanied by concentration variations. This bypass flow is closely linked to the fluidizing behaviour and parameters discussed in Chapter 3.3 such as the amount, size distribution and density of the bed material as well as the fluidizing velocity and the size of the combustion chamber. This makes an comparison with other test facilities even more complicated as illustrated by Fig. 4.1.2 where the oxygen profiles from two small lab-scale

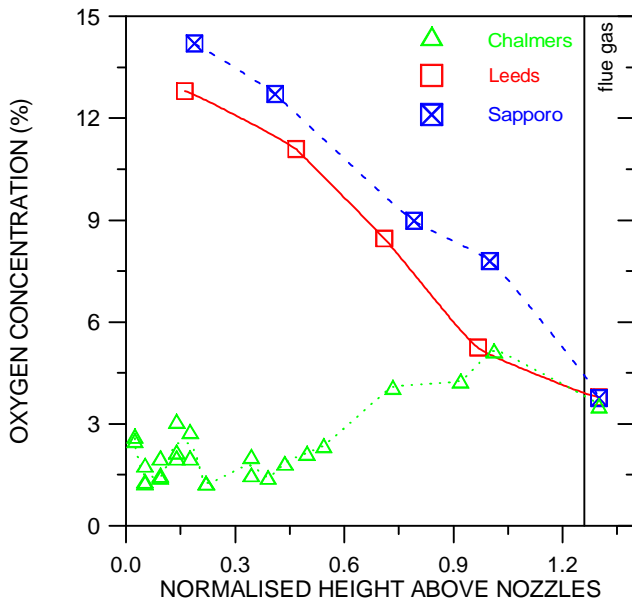


Fig. 4.1.2 Comparison of the vertical profiles of oxygen along the centre line in the combustion chamber between the Chalmers boiler and two lab-scale CFB test units. Fuel: Bituminous coal. Test conditions: See Table 4.1.1. Input data: [Fig4_1_2.xls](#)

facilities, Hirama et al., 1987 and Wang et al., 1994 is re-plotted together with the centre line data for the Coal2 test in the Chalmers boiler. A striking difference between the data from the three facilities are the high oxygen concentrations in the lower part of the combustion chamber for the two small test facilities in comparison to the Chalmers data. As a first guess, the reason for this difference could lie in the slim geometry of the lab-scale facilities in Leeds and Sapporo. However, this is contradictory to the results obtained in the Hamburg unit, Fig. 4.1.1. Instead, the smaller bed material size in combination with less amount of material circulating in the loop (which causes less pressure drop across the riser), Table 4.1.1, could lead to the situation that no bottom bed was formed and no fuel was burned in the lower regions in the Leeds and Sapporo units. The presence of a bottom bed is crucial for the bypass flow of air to the splash zone where it mixes with the volatiles.

4.2 Flows of Char

The curves of the cumulative char content (Figs 3.3.4.1, 3.3.4.2, 3.3.7.1 and 3.3.7.2) are the results of a steady-state calculation of the char distribution in the combustion chamber. This should be compared with the flows of char entering and leaving the combustion chamber. The data for this calculation are given in Table 4.2.1. The total flow of solids leaving the combustion chamber is estimated using the expression $G_{\text{exit}} = 0.5 \cdot \sigma_{\text{exit}} \cdot (u - u_t)$ [kg solids/m², s] taken from Johnsson et al., 1997. u is the fluidisation velocity at the top of the combustion

	Chalmers	Leeds	Sapporo	Hamburg
Height of riser sect. (m)	10.8	6.2	5.0	15.5
Cross-section area (m ²)	2.37	0.020	0.0038	0.0078
Bed material	Silica sand	Silica sand	Silica sand	Silica sand
Size of bed material (µm)	320	120	200	320
Fluidizing velocity (m/s)	5.7	5.2	7.9	7.0
DP total across riser (kPa)	6.6	1.2	2.8	7.0
Excess air ratio	1.21	1.25	1.20	1.20
Bed temperature (°C)	850	830	800	850
Sec. air/tot. air	0.35	0.40	-	0.40
Inj. level sec. air (m)	2.2	1.3	-	3.2
Reference	This paper	Wang et al., 1994	Hirama et al., 1987	Knöbig et al., 1997

chamber and u_t the terminal velocity for the average particle size for the sample taken at 7.9 meter above the bottom of the combustion chamber. Without the factor 0.5, the expression assumes that the particles measured at the top as σ_{exit} are actually leaving the combustion chamber. However, only part of the cross-sectional average solids concentration is moving upwards in the core region towards the hot cyclone. Measurements by Zhang et al., 1993 showed that the solids concentration in the core region is about half the cross-sectional average concentration. The calculation still does not take into account the fact that part of the particles measured in the core region may not reach the hot cyclone. This ratio between the amount of particles present in the core region at the top of the combustion chamber and the amount entering into the hot cyclone is still unknown and neglected in the below calculations. The vertical profiles of the solids concentrations (Figs 3.3.1.2 and 3.3.5.2) together with a cross-section of 1.78 m², representing the core region, permits an estimation of the flows of solids to the hot cyclone with the limitation mentioned above. By using the char concentrations at a height of 12 meter in Fig 3.3.6.1, the char flows to the cyclone for the three fuel cases were calculated. This flow of char re-enters into the combustion chamber and should be compared to the fresh flow of combustibles in the fuel supplied. The ratio between the re-entering cyclone flow of combustibles and the fresh fuel flow is calculated to 0.37-0.95. The large difference between the three coal cases is due to the different values of the solids concentration in the top of the combustion chamber discussed in chapter 3.3.1. The coal case closest to the conditions of the peat1 and wood1 cases has a ratio of combustibles of 0.37 to be compared with 0.08 for peat and 0.04 for wood, Table 4.2.1.

	Coal1	Coal2	Coal3	Peat1	Wood1
Fluidizing velocity in the top of the comb. chamber (m/s)	6.45	6.17	6.39	6.68	6.84
Solids concentration in the top of the comb. chamber (kg solids/m ³)	6.0	8.0	3.0	4.0	3.0
Flow of solids through the hot cyclone (tonnes/h)	83	103	41	58	43
Char concentration in flow of solids through the hot cyclone (%)	1.0	1.0	1.0	0.2	0.18
Flow of combustibles through the hot cyclone (tonnes/h)	0.83	1.03	0.41	0.12	0.08
Flow of combustibles in the fuel to the comb. chamber (tonnes/h)	1.14	1.09	1.09	1.44	1.80
Ratio combustibles from hot cyclone to combustibles in the fuel	0.73	0.95	0.37	0.08	0.04

Apart from the external recirculation of char an internal flow of combustibles also contributes to the mass balance of char entering into the bottom part of the combustion chamber. Based on extensive measurements of the wall-region (both mass-flows and analysis of samples taken), an estimation of this flow is possible (Johnsson et al., 1997) for a similar coal case as Coal2. A schematic illustration of the

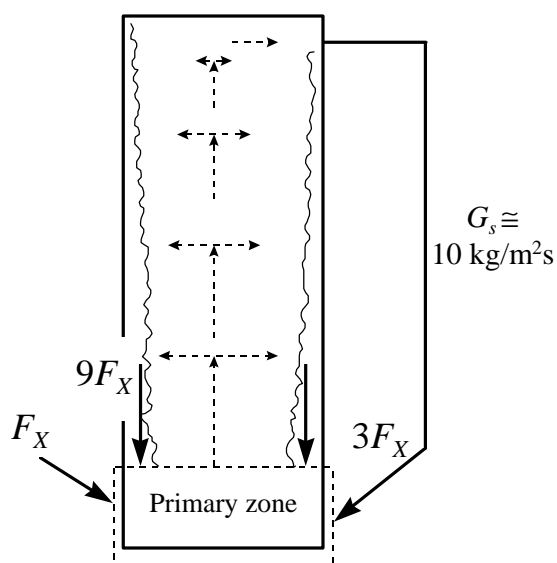


Fig. 4.2.1 Schematic illustration of the solid fluxes in the furnace. Char flows related to char with fuel. Adopted from Johnsson et al., 1997.

results is given in Fig. 4.2.1. From this figure it can be seen that the internal char flow is about three times higher than the external char flow. In this particular case the external char flow was calculated to about three times the flow of combustibles as fuel which is much more than the Coal2 case in Table 4.2.1. The reason for this difference is that a char concentration of about 4.5% was used for the solid flow from the hot cyclone by Johnsson et al., 1997 compared to only about 1% for the three coal cases in this report based on the evaluation of the data given in Fig. 3.3.2.1. In this figure the large scatter in data is obvious. This scatter results in a large uncertainty when using an analysis of a single sample. A second reason for the difference in char content could be that during the tests reported by Johnsson et al., 1997 the boiler was operated on a sieved bituminous coal with no size fractions greater than 10mm present in the fuel feed. The surface weighted average particle size of the char fraction in the samples taken at the 7.9 meter level were 0.74mm, 0.71mm and 0.58mm (Fig. 3.3.3.3) for the Coal1 and Coal 3 cases, while only 0.16mm was obtained for a similar sample given by Johnsson et al., 1997. This means that, due to a smaller average char particle size, more char can be expected to be carried over to the cyclone, increasing the char content in the particle flow from the hot cyclone compared to an operating case having larger char particles .

5. CONCLUSIONS

The results presented together with the evaluation of data permit the following conclusions regarding the combustion of coal, peat and wood in the 12 MW CFB boiler at Chalmers University of Technology:

- Much higher oxygen concentrations were measured in the combustion chamber for peat and wood compared to coal and much more combustion takes place in the volume just upstream of the cyclone and/or in the cyclone in the peat and wood cases compared to coal.
- Large variations of the oxygen concentrations over the cross-section for all three fuels is explained as an effect of insufficient penetration depth of secondary air in combination with partial plugging of some of the secondary air nozzles.
- The char loading during peat and wood combustion was 12 and 3% respectively of the amount found during coal combustion.
- Burning of the high volatile fuels peat and wood, caused much lower concentrations of oxygen close to the front wall, where the fuel supply is located, compared to regions close to the back wall.
- For all fuels more than 80% of the mass of char is retained in the bottom bed and splash zone below 2 meter from the air distributor of the combustion chamber.
- The amount of char returning from the cyclone leg and particle seal to the bottom bed in relation to the flow of combustibles added as fuel, drops from 0.4 in the Coal3 case to 0.08 for peat and 0.04 for wood.
- Using the gas concentration measurements in comparison with the evaluation of the char loading leads to different results regarding the combustion and conversion of the fuel in the coal case. The reason for this discrepancy is a bypass flow (or through-flow) of gas bypassing the bottom bed with a high oxygen content, a gas bypassing the bottom bed with a much higher velocity than the remaining gas flow.

6. ACKNOWLEDGEMENT

This work has been supported financially by the Swedish National Board for Technical and Industrial Development (NUTEK). The operation of the research equipment at the boiler by Abbas Zarrinpour and Hans Schmidt is gratefully acknowledged.

7. REFERENCES

Hirama, T., Takeuchi, H., Horio, M., 1987, *Nitric Oxide Emission from Circulating Fluidized-Bed Coal Combustion*, Proceedings of the Ninth International Conference on Fluidized Bed Combustion, (Ed. J. P. Mustonen), The American Society Of Mechanical Engineers, New York, pp. 898-905.

Johnsson, F., Leckner, B., 1995, *Vertical Distribution of Solids in A CFB-Furnace*, Proceedings of the Thirteenth International Conference on Fluidized Bed Combustion, (Ed. K. J. Heinschel), The American Society Of Mechanical Engineers, New York, pp. 671-679.

Johnsson, F., Breitholtz, C., Leckner, B., 1997, *Solids Segregation in a CFB-Boiler Furnace*, Fluidization IX, Engineering Foundation Durango, 1998.

Karlsson, M., Åmand, L.-E., Leckner, B., 1996, *Comparison of FTIR and DOAS Measurement of NH₃ and NO in Fluidized Bed Combustion Gases*, Proceedings of the Finnish-Swedish Flame Days, IFRF, September 3-4, Naantali, Finland.

Knöbig, T, Werther, J., Åmand, L.-E. , Leckner, B., 1997, *Are Measurements in Small-Scale Units Representative of the Performance of Large-Scale Combustors with Circulating Fluidized Beds?*, VDI-Bericht 1314 entitled: Wirbelschichtfeuerungen: Erfahrungen und Perspektiven, VDI Verlag, Düsseldorf.

Lyngfelt, A., Åmand, L.-E., Leckner, B. 1995, *Low N₂O and SO₂ Emissions from Circulating Fluidized Bed Boilers*, Proceedings of the Thirteenth International Conference on Fluidized Bed Combustion, (Ed. K. J. Heinschel), The American Society Of Mechanical Engineers, New York, pp. 1049-1057.

Lyngfelt, A., Åmand, L.-E., Leckner, B. 1996, *Progress of Combustion in the Furnace of a Circulating Fluidized Bed Boiler*, Proceedings of the Twenty-Sixth Symposium (International) on Combustion, The Combustion Institute, Pittsburgh, pp. 3253-3259.

Mattisson, T., Lyngfelt, A., 1995, *The Presence of CaS in the Combustion Chamber of a 12 MW Circulating Fluidized Bed Boiler*, Proceedings of the Thirteenth International Conference on Fluidized Bed Combustion, (Ed. K. J. Heinschel), The American Society Of Mechanical Engineers, New York, pp. 819-829.

Zhang, W., Johnsson, F., Leckner, B., 1993, *Characteristics of the Lateral Particle Distribution in Circulating Fluidized Bed Boilers*, *Circulating Fluidized Bed Technology IV*, (Ed. A. A. Avidan), AIChE, Somerset, pp. 266-273.

Åmand, L.-E., Leckner, B., Andersson, S., 1991, *Formation of N₂O in Circulating Fluidized Bed Boilers*, *Energy & Fuels*, **5**, pp. 815-823.

Åmand, L.-E., Leckner, B., 1993, *Reduction of N₂O in a Circulating Fluidized Bed Combustor*, *Fuel*, **73**, pp.1389-1397.